THE JOURNAL OF BIOLOGICAL CHEMISTRY VOL. 286, NO. 16, pp. 14435–14444, April 22, 2011

Lacrimal Gland Development and Fgf10-Fgfr2b Signaling Are Controlled by 2-*O*- and 6-*O*-sulfated Heparan Sulfate*

Received for publication, January 26, 2011, and in revised form, February 25, 2011 Published, JBC Papers in Press, February 28, 2011, DOI 10.1074/jbc.M111.225003

Xiuxia Qu[‡], Christian Carbe[‡], Chenqi Tao[‡], Andrea Powers[‡], Roger Lawrence[§], Toin H. van Kuppevelt[¶], Wellington V. Cardoso[‖], Kay Grobe[**], Jeffrey D. Esko[§], and Xin Zhang[‡1]

*From the [‡]Department of Medical and Molecular Genetics, Indiana University School of Medicine, Indianapolis, Indiana 46202, the [¶]Department of Biochemistry, Radboud University Nijmegen Medical Centre, Nijmegen Centre for Molecular Life Sciences, P. O. Box 9101, 6500 HB, Nijmegen, The Netherlands, [‖]Pulmonary Center, Boston University School of Medicine, Boston, Massachusetts 02118, **Physiological Chemistry and Pathobiochemistry, University of Muenster, 48149 Münster, Germany, and the [§]Department of Cellular and Molecular Medicine, Glycobiology Research and Training Center, University of California San Diego, La Jolla, California 92093*

Heparan sulfate, an extensively sulfated glycosaminoglycan abundant on cell surface proteoglycans, regulates intercellular signaling through its binding to various growth factors and receptors. In the lacrimal gland, branching morphogenesis depends on the interaction of heparan sulfate with Fgf10-Fgfr2b. To address if lacrimal gland development and FGF signaling depends on 2-*O*-sulfation of uronic acids and 6-*O*-sulfation of glucosamine residues, we genetically ablated heparan sulfate 2-*O* and 6-*O* sulfotransferases (*Hs2st*, *Hs6st1*, and *Hs6st2*) in developing lacrimal gland. Using a panel of phage display antibodies, we confirmed that these mutations disrupted 2-*O* and/or 6-*O* but not *N*-sulfation of heparan sulfate. The *Hs6st* mutants exhibited significant lacrimal gland hypoplasia and a strong genetic interaction with *Fgf10*, demonstrating the importance of heparan sulfate 6-*O* sulfation in lacrimal gland FGF signaling. Altering *Hs2st* caused a much less severe phenotype, but the *Hs2st*;*Hs6st* double mutants completely abolished lacrimal gland development, suggesting that both 2-*O* and 6-*O* sulfation of heparan sulfate contribute to FGF signaling. Combined *Hs2st*;*Hs6st* deficiency synergistically disrupted the formation of Fgf10-Fgfr2b-heparan sulfate complex on the cell surface and prevented lacrimal gland induction by Fgf10 in explant cultures. Importantly, the *Hs2st*;*Hs6st* double mutants abrogated FGF downstream ERK signaling. Therefore, Fgf10-Fgfr2b signaling during lacrimal gland development is sensitive to the content or arrangement of *O*-sulfate groups in heparan sulfate. To our knowledge, this is the first study to show that simultaneous deletion of *Hs2st* and *Hs6st* exhibits profound FGF signaling defects in mammalian development.

Heparan sulfate is a cell-surface glycosaminoglycan playing important roles in the transport and signaling of multiple growth factors, including Hedgehog, Wnt, bone morphogenic protein (BMP), and fibroblast growth factor (FGF) (1–3). Heparan sulfate is first synthesized from the activated monosaccharides, UDP-glucuronic acid and UDP-*N*-acetylglucosamine, by an Ext copolymerase complex to form a copolymer of glucuronic acid and *N*-acetylglucosamine. Polymerization is followed by *N*-deacetylation/*N*-sulfation of subsets of *N*-acetylglucosamine residues by *N*-deacetylase-*N*-sulfotransferase (Ndst)[2] enzymes (4). Because of the incomplete processing by the Ndst enzymes, the polysaccharide backbone is divided into stretches of variable length of *N*-sulfated disaccharides (NS domains) and *N*-acetylated disaccharides (NA domains). A portion of the D-glucuronic acid residues in the NS domains is next converted by glucuronyl C5-epimerase (Hsepi) into L-iduronic acids. A 2-*O*-sulfotransferase (Hs2st) transfers a sulfate group to the C-2 carbon of the iduronic acids and less frequently to glucuronic acid. Finally, 6-*O*-sulfotransferases (Hs6st) and more rarely 3-*O*-sulfotransferases (Hs3st) add sulfate groups to the C-6 and C-3 carbon of the glucosamine residues, respectively. These reactions do not go to completion, leading to great structural complexity within the NS domains. Additional complexity of heparan sulfate can be generated at the cell surface, as membrane-bound Sulf1 and Sulf2 specifically remove a subset of 6-*O* sulfates from heparan sulfate, whereas extracellular heparanase can cleave and release fragments of the heparan sulfate chain.

The interaction of heparan sulfate with FGF and FGF receptors is still under considerable scrutiny (5–14). At least *in vitro*, the FGF family proteins and their receptors often bind with increasing affinity to more highly sulfated heparan sulfates, suggesting a lack of specificity with respect to the precise arrangement of *N*-, 2-*O*, and 6-*O* sulfate groups (11, 15, 16). In *Drosophila*, tracheal branching morphogenesis depends on FGF signaling mediated by the interaction of the FGF homolog *branchless* with the FGF receptor, *breathless*. Mutating individually *Hs2st* and *Hs6st* genes apparently causes minimum consequences in trachea branching morphogenesis (17). However, strong trachea defects are revealed in *Hs2st*:*Hs6st* double mutants, demonstrating that the 2-*O*-sulfate and 6-*O*-sulfate groups are individually dispensable for heparan sulfate function in FGF signaling in this system. These observations and the

* This work was supported, in whole or in part, by National Institutes of Health Grants EY018868 (to X. Z.) and GM33063 and GM93131 (to J. D. E.). This work was also supported by the Ralph W. and Grace M. Showalter Research Trust Fund (to X. Z.).

[1] To whom correspondence should be addressed. Tel.: 317-274-1062; Fax: 317-274-1069; E-mail: xz4@iupui.edu.

[2] The abbreviations used are: Ndst, *N*-deacetylase-*N*-sulfotransferase; NS domain, *N*-sulfated disaccharide domain; NA domain, *N*-acetylated disaccharide domain; LACE, ligand and carbohydrate engagement; MEF, mouse embryonic fibroblast; FGFR, FGF receptor.

related finding that many organs that depend on heparan sulfate appear to develop normally in mutants lacking individual sulfotransferases (18–21) have led to the idea that the interaction of FGFs and FGF receptors with heparan sulfate shows little specificity.

In counterpoint to this conclusion, other studies have pointed to specificity in the interaction of some FGF family members with their receptors. Binding studies of oligosaccharides to FGFs showed that Fgf10 requires 6-*O*-sulfate but not 2-*O*-sulfate groups, whereas Fgf2 requires only 2-*O*-sulfate and *N*-sulfate groups (22). The selectivity of FGF becomes even more pronounced when presented in a complex with FGFR and endogenous heparan sulfate in mouse embryos. Using a ligand and carbohydrate engagement assay (LACE), Allen and Rapraeger (23) have shown that 2-*O*-sulfation of heparan sulfate is required for Fgf1-Fgfr2b binding but not for Fgf1 or Fgf1-Fgfr2c binding. Heparan sulfate 2-*O* and 6-*O*-sulfation was found to promote Fgf10-mediated end budding or duct elongation in submandibular gland culture, and distinct organ specific phenotypes were observed *in vivo* when murine 2-*O* and 6-*O*-sulfation genes, *Hs2st* and *Hs6st1*, were mutated (18, 20, 24–27). Similarly, we have shown in lens development that a lack of heparan sulfate *N*-sulfation disrupts its interaction with Fgf8b-Fgfr3c but not with the Fgf8b-Fgfr3b pair (28). We recently showed that *N*-sulfated heparan sulfate is highly enriched in the lacrimal gland bud, which potentiates a restricted activation of FGF signaling during lacrimal gland outgrowth (29). Taken together, these findings suggest that FGF signaling is sensitive to the positional distribution of sulfate groups in the heparan sulfate chains.

In this study we took a similar approach taken by Kamimura *et al.* (17) in their study of FGF signaling in *Drosophila* and investigated the role of heparan sulfate sulfation sequence in lacrimal gland development in mice by deleting *Hs2st* and *Hs6st* genes. In contrast to the lack of branching morphogenesis defects in the *Drosophila Hs6st* mutants, we showed that the loss of murine *Hs6st* significantly disrupted lacrimal gland formation. The *Hs2st* mutant phenotype was much weaker, but the *Hs2st*:*Hs6st* double mutants completely abolished lacrimal gland development. These results demonstrated that vertebrate FGF signaling in the lacrimal gland indeed depends on specific sulfation of the chains.

EXPERIMENTAL PROCEDURES

Mice—*Hs6st1*^{flox} and *Hs2st*^{flox} mice have been previously described (20, 27). *Hs6st2*^{KO} mice were obtained from Lexicon Genetics via Mutant Mouse Regional Resource Centers (MMRRC:011715-UCD). *Fgf10*$^{+/-}$ mice were kindly provided by Dr. Hisashi Umemori (University of Michigan, Ann Arbor, MI) (30). *Le-Cre* mice were kindly provided by Dr. Ruth Ashery-Padan (Tel Aviv University, Tel Aviv, Israel) and Dr. Richard Lang (Children's Hospital Research Foundation, Cincinnati, OH) (31). All experiments were performed in accordance with institutional guidelines.

Immunohistochemistry and RNA in Situ Hybridization—Immunohistochemistry was performed on cryosections or paraffin sections as previously described (28, 29). For phospho-ERK staining, the Tyramide Signal Amplification kit (TSA™ Plus System, PerkinElmer Life Sciences, Waltham, MA) was used to amplify the signal (32). The antibodies used were anti-phospho-ERK1/2 (#9101, Cell Signaling Technology, Beverly, MA) and anti-phosphohistone H3 (#06–570, Upstate Biotechnology, Temecula, CA). TUNEL assays were performed on 10-μm paraffin sections following the manufacturer's instructions in the In Situ Cell Death Detection kit (Roche Applied Science, Indianapolis, IN). Cell proliferation and apoptosis rates were calculated as the ratio of phosphohistone H3 or TUNEL-positive cells against DAPI-positive cells, and results were analyzed by one-way analysis of variance.

A series of phage-display derived antibodies with VSV-tag were used to detect specific modifications of heparan sulfate in tissue sections (33). Cryo-sections were hydrated in PBS for 10 min, quenched of peroxidase activity by 3% H_2O_2 and 10% methanol in PBS solution, and then blocked with 2% BSA in PBS at room temperature for 1 h followed by incubation with phage-display-derived antibodies (1:1–1:5 diluted with 0.2% BSA/PBS) at 4 °C overnight. After PBS washing 3 times, sections were incubated with rabbit anti-VSV antibody (#563, MBL, Woburn, MA) for 2 h at room temperature and rinsed in PBS before a 1-h incubation with HRP-labeled anti-rabbit antibody. The signal was amplified and detected using Tyramide Signal Amplification kit. The total heparan sulfate was detected using 3G10 antibody (Seikagaku, Tokyo, Japan) after the section was treated with heparitinase I.

RNA *in situ* hybridization on cryosections was performed according to a standard protocol (29). The following probes were used: *Erm* (from Dr. Bridget Hogan, Duke University Medical Center, Durham, NC), *Hs6st1*, *Hs6st2*, and *Hs6st3* (34). *Hs2st* probe was generated from a full-length cDNA clone (IMAGE: 6849136, Open Biosystems, Huntsville, AL). At least three embryos of each genotype were analyzed for each probe.

FGF-FGFR Complex Binding Assay—The binding of the FGF-FGFR complex with heparan sulfate was examined using the LACE assay as previously described (28, 29). Briefly, 10 μm paraffin sections of the mutant embryos and their matched littermates were deparaffinized and rehydrated followed by incubation in 0.5 mg/ml sodium borohydride for 10 min and in 0.1 M glycine for 30 min and then blocked with 2% BSA for 1 h at room temperature. Next, the sections were incubated with a mixture of 20 μM FGF and 20 μM human FGFR-Fc chimera (both from R&D Systems, Minneapolis, MN) in RPMI 1640 with 10% FBS at 4 °C overnight. After rinsing three times with PBS, the slides were incubated with cy3-labeled anti-human Fc IgG antibody for 2 h at room temperature. The fluorescent signal was examined using a Leica DM500 fluorescent microscope.

Explant Culture—Lacrimal gland explant cultures were carried out with E13.5-E14.5 embryos as described (29). Briefly, 80–120-μm diameter heparin acrylic beads (Sigma) were washed in PBS and incubated with 250 μg/ml recombinant FGF10 (R&D Systems) or 5 mg/ml BSA in PBS at 4 °C overnight. The whole eye with ectoderm and surrounding mesenchyme was dissected and laid flat on a filter paper (Nitrocellulose Membrane Black Gridded, 0.45 μm pore, Millipore, Billerica, MA). After FGF10- or BSA-soaked beads were punched into the periocular mesenchyme by forceps, the tissue

on top of the filter was floated in the culture medium (CMRL-1066 supplemented with 10% FBS, 4 mM L-glutamine, 0.1 mM nonessential amino acids, and antibiotics (Invitrogen, Carlsbad, CA)). Explants were cultured for 48 h in a 37 °C humidified incubator with 5% CO_2, and the GFP expressing lacrimal gland buds were examined and photographed under a Leica MZ16F dissecting microscope.

Mouse Embryonic Fibroblast (MEF) Cells—Primary MEF cells were isolated from embryos at the E13.5 to E14.5 stage. Briefly, the uterine horns were dissected from pregnant females and rinsed in 70% (v/v) ethanol before transfer into sterilized PBS. After the heads and the internal organs were cut away, the trunks were washed with fresh PBS to remove blood cells, finely minced into small pieces in a minimal amount of PBS, and digested in 1–2 ml of 0.25% trypsin-EDTA for 10 min at 37 °C under gentle agitation. The supernatant was combined with 2 volumes of fresh Dulbecco's modified Eagle's medium (DMEM) and centrifuged at a low speed (400 × *g*). The cell pellet was resuspended in DMEM containing 10% FBS and antibiotics (penicillin G/streptomycin) and cultured in a humidified 5% CO_2 incubator at 37 °C. MEFs from the second passage were infected with Ad5CMVCre (Gene Transfer Vector Core, University of Iowa, IA) overnight at multiplicity of infection 100 plaque-forming units/cell and cultured for 2 more days after replacing with fresh culture medium.

MEF cells were immortalized by SV40 large T antigen (SV40-T) as previously described (35, 36). Briefly, SV40-T expressing retrovirus was collected from the supernatant of the ψ2 producer cells kindly provided by Lawrence A. Quilliam (Indiana University School of Medicine, Indianapolis, IN) and filtered (0.45 μm). The primary MEF cells were infected by SV40-T retrovirus and selected with 100 μg/ml hygromycin for about 10 days. Drug-resistant cells were cloned by serial dilution and two or more clones were expanded for each genotype.

FGF10-induced Cell Signaling and Western Blot Analysis—The Ad5CMVCre virus-infected MEF cells were seeded in 24-well plates at 1 × 10^5 cells/well and further cultured in DMEM with 10% FBS and antibiotics for 24 h. After the cells were treated in DMEM containing 0.4% FBS for 12 h and serum-free DMEM containing 0.1% BSA for an additional 24 h, FGF10 was added into the wells at a 10 ng/ml final concentration for 1, 2.5, 5, 7.5, 10, and 15 min at 37 °C. The medium was immediately discarded, and the cells were washed with cold PBS twice before being lysed in 100 μl of lysis buffer (50 mM Tris-HCl, pH 8.0, 150 mM NaCl, 1% Nonidet P-40, 0.5% sodium deoxycholate, 0.1% SDS, 1 mM EDTA, 1 mM sodium vanadate) with protease and phosphatase inhibitors (Pierce). After centrifugation at 10,000 × *g* for 15 min at 4 °C, 30 μg of cell lysate protein was analyzed by SDS-PAGE (12% gels) and transferred to Millipore Immobilon FL PVDF membranes (Millipore). The membranes were blocked in Odyssey blocking buffer for 1 h with gentle shaking followed by an overnight incubation in the mixture of mouse anti-phospho-ERK1/2 (sc-7383, Santa Cruz Biotechnology, Santa Cruz, CA) and rabbit anti-ERK1/2 (#4695, Cell Signaling Technology) antibodies. After rinsing with PBS-T (0.1% Tween 20 in PBS) 3 times at 4 °C, the blots were incubated with IRDye-linked anti-mouse and anti-rabbit secondary antibodies for 1 h and washed 3 times with PBST and twice with PBS. The membrane was scanned in an Odyssey SA scanner (LICOR Biosciences, Lincoln, NE), and band intensities were quantified using the Odyssey software.

Heparan Sulfate Disaccharide Compositional Analysis—Disaccharide analysis of heparan sulfate extracted from primary MEFs was carried out using procedures previously described (37). Briefly, heparan sulfate was extracted from MEF cell pellets by exhaustive digestion with Pronase (Sigma) in PBS at 37 °C for 24 h followed by anion-exchange chromatography (DEAE-Sephacel, GE Healthcare). Heparan sulfate was eluted with 1 M NaCl and desalted by gel filtration (PD-10, GE Healthcare). All preparations were digested with 1 milliunit each of heparin lyases I, II, and III (IBEX, Montreal) for 16 h at 37 °C in 50 μl of buffer containing 40 mM ammonium acetate and 3.3 mM calcium acetate, pH 7. Heparan sulfate disaccharides were then tagged with [$^{12}C_6$]aniline. For compositional analysis, each sample was mixed with an equimolar amount of [$^{13}C_6$]aniline-tagged disaccharide standards. Aniline-derivatized disaccharides were separated on a C18 reversed-phase column (Phalanx 1 × 150-mm micro-bore, 5 μm, Higgins Analytical) with 5 mM concentrations of the ion pairing agent dibutylamine (Sigma) and 8 mM acetic acid, operated at a flow rate of 50 μl/min. Disaccharides with higher sulfation were eluted with increasing methanol concentration using a step gradient produced on a Dionex U3000 capillary HPLC and analyzed in tandem by a LTQ Orbitrap mass spectrometer (Thermo, San Jose, CA). Data were analyzed with the Xcalibur software supplied with the mass spectrometer.

RESULTS

Hs2st and Hs6st Are Required for Lacrimal Gland Development—Lacrimal gland development is an excellent model for studying the role of heparan sulfate in FGF signaling (29, 38, 39). Arising from the conjunctival epithelium at the temporal side of the eye, the budding of the lacrimal gland is critically dependent on Fgf10 expressed in the periocular mesenchyme (40, 41). Heparan sulfate 2-*O* sulfotransferase (*Hs2st*) and two of the heparan sulfate 6-*O* sulfotransferases (*Hs6st1* and *-2*) were detected in the E14.5 lacrimal gland bud by RNA *in situ* hybridization using their antisense probes (Fig. 1, *A–D*). As a control, no signal was observed with the corresponding sense probes (data not shown). We, thus, generated the lacrimal gland-specific ablations of *Hs2st* and *Hs6st1/2* genes using the *Le-Cre* driver, which we have previously shown to express both Cre recombinase and GFP reporter in the lacrimal gland epithelium (29). At E14.5, when lacrimal gland buds became visible in the wild type embryos (Fig. 1*E*), no obvious defects were observed in the *Le-Cre;Hs2st*$^{flox/flox}$ (hereafter referred as *Hs2st*^{CKO}) (Fig. 1*F*), the *Le-Cre;Hs6st1*$^{flox/flox}$, and the *Hs6st2*$^{-/-}$ mutants (data not shown). In contrast, many of the *Le-Cre;Hs6st1*$^{flox/flox}$*;Hs6st2*$^{-/-}$ (hereafter referred as *Hs6st*^{CKO}) mutant embryos exhibited stunted (47%) or even no (17%) lacrimal gland bud (Fig. 1, *G* and *M*). The most severe phenotype was observed in the *Le-Cre;Hs2st*$^{flox/flox}$*; Hs6st1*$^{flox/flox}$*;Hs6st2*$^{-/-}$ (hereafter referred as *Hs2st*^{CKO}*; Hs6st*^{CKO}) mutants, where the majority (61%) of the embryos lack lacrimal gland bud at E14.5 (Fig. 1, *H* and *M*). At birth, 50% of the *Hs2st*^{CKO} mutants also exhibited diminutive lacrimal

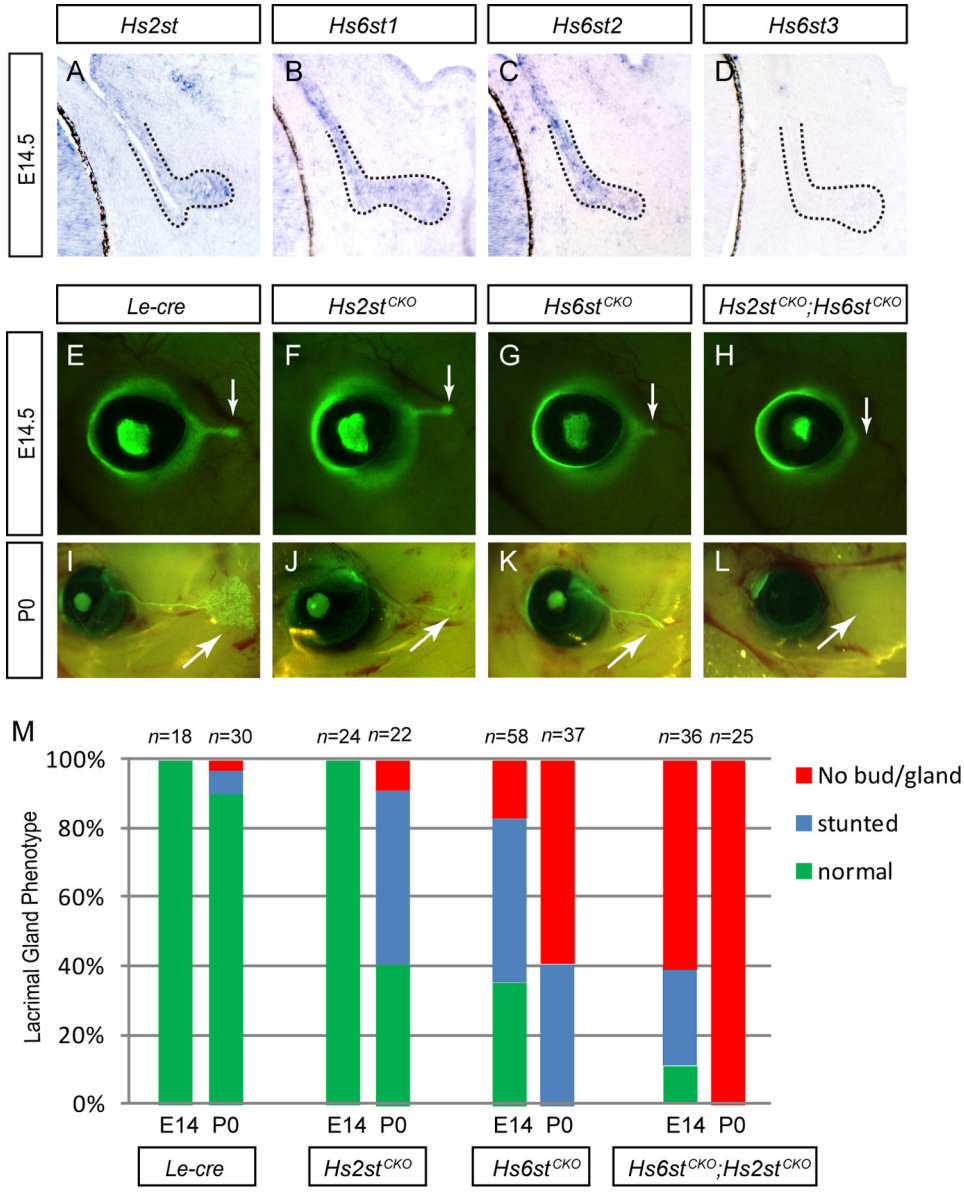

FIGURE 1. **Heparan sulfate 2-*O* and 6-*O* sulfotransferases are required for lacrimal gland branching morphogenesis.** *A–D*, lacrimal gland bud (*broken line*) expressed *Hs2st*, *Hs6st1*, and *Hs6st2* but not *Hs6st3* as shown by RNA *in situ* hybridization. *E–L*, compared with the wild type control (*Le-Cre*), lacrimal gland budding at E14.5 was normal in the *Hs2st* mutant ($Hs2st^{CKO}$), stunted in the *Hs6st1*/*Hs6st2* mutant ($Hs6st^{CKO}$), and mostly disrupted in the *Hs2st*/*Hs6st1*/*Hs6st2* mutant ($Hs2st^{CKO}$;$Hs6st^{CKO}$). At P0, progressive loss lacrimal gland was observed in all three mutants (*arrows*). *M*, quantification of the lacrimal gland phenotypes is shown.

glands with few side branches, whereas 59% of the $Hs6st^{CKO}$ and 100% of the $Hs2st^{CKO}$;$Hs6st^{CKO}$ completely lost lacrimal glands (Fig. 1, *I–M*). Therefore, ablation of *Hs6sts* resulted in significantly more severe phenotype than that of *Hs2st*, but *Hs2st* and *Hs6st* also exhibited genetic synergy in lacrimal gland branching morphogenesis.

Disruption of Heparan Sulfate O-Sulfation in the Hs2st and Hs6st Mutants—To determine whether the mutations affected heparan sulfate composition *in situ*, we stained tissue sections with mAb 3G10 after heparinase digestion, which creates a neoepitope in place of each chain. 3G10 antibody staining was unchanged in all lacrimal gland buds (Fig. 2, *A–D*), indicating that altering sulfation *per se* did not affect the number of heparan sulfate chains in the tissue. We next used a panel of phage-display antibodies to examine the sulfation patterns of heparan sulfate in the mutants. The first step in heparan sulfate modification catalyzed by Ndst is the formation of *N*-sulfated glucosamine residues, which can be recognized by the HS4E4V antibody (42). As expected, the HS4E4V staining was preserved in the *Hs2st* and *Hs6st* mutants (Fig. 2, *E–H*). In contrast, the AO4B08 staining, which was reported to require *N*-, 2-*O*-, and 6-*O*-sulfated heparan sulfate, was abolished in all *Hs2st* and *Hs6st* mutants (Fig. 2, *I–L*) (42). Therefore, altering *Hs2st* and *Hs6st* resulted in loss of 2-*O* and 6-*O* sulfation but not *N*-sulfation. EV3C3V antibody was reported to require *N*- and 2-*O*-sulfated heparan sulfate epitopes (43), and it strongly stained the basement membrane of the wild type and $Hs6st^{CKO}$ lacrimal gland buds but not that of the $Hs2st^{CKO}$ and $Hs2st^{CKO}$;$Hs6st^{CKO}$ mutants (Fig. 2, *M–P*). Finally, using RB4EA12, which was reported to be specific for *N*- and 6-*O*-sulfate groups (43),

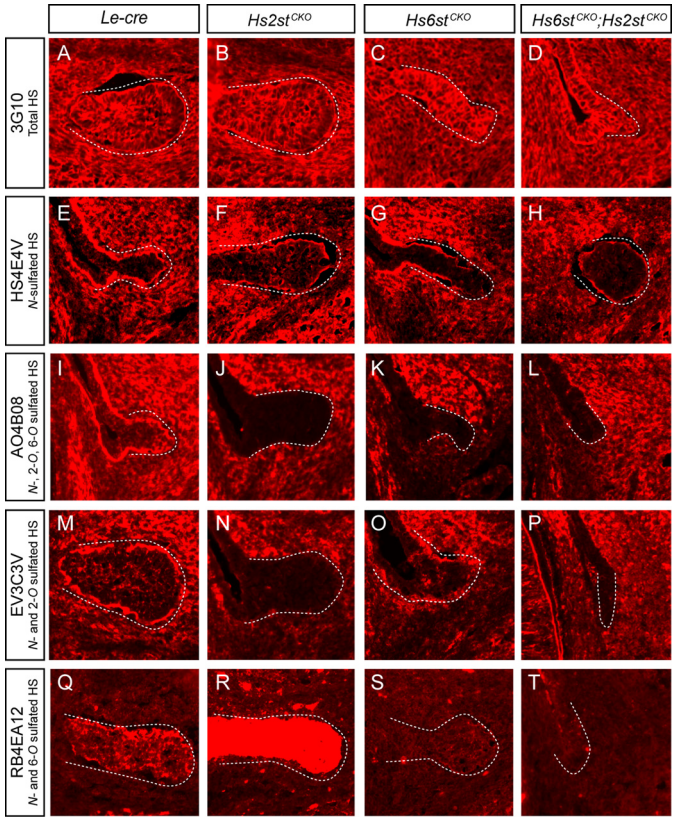

FIGURE 2. **Hs2st and *Hs6st* ablations disrupted heparan sulfate *O*-sulfation modification.** 3G10 antibody detected a similar amount of heparan sulfate chains in all lacrimal gland primordia (*A–D*), and HS4E4V antibody staining indicated that *N*-sulfated heparan sulfate was not lost in the *Hs2st* and *Hs6st* mutants (*E–H*). In contrast, all mutants lost AO4B08 (2-*O*-and 6-*O*-sulfated heparan sulfate) staining (*I–L*). These results showed that *Hs2st* and *Hs6st* ablations indeed resulted in heparan sulfate *O*-sulfation defects. Finally, EV3C3V (*N*- and 2-*O*-sulfated heparan sulfate) staining was specifically lost in the $Hs2st^{CKO}$ and $Hs2st^{CKO}$;$Hs6st^{CKO}$ mutants (*M–P*), and RB4EA12 (*N*- and 6-*O*-sulfated heparan sulfate) staining revealed 6-*O*-sulfated heparan sulfate was lost in the $Hs6st^{CKO}$ mutants but up-regulated in the $Hs2st^{CKO}$ mutants (*Q–T*).

we observed that heparan sulfate 6-*O* sulfation was lost in the $Hs6st^{CKO}$ and the $Hs2st^{CKO}$;$Hs6st^{CKO}$ mutants but strongly elevated in the $Hs2st^{CKO}$ mutants (Fig. 2, *Q–T*). These results showed that *Hs2st* and *Hs6st* mutations indeed disrupted the addition of 2-*O* and 6-*O* sulfate groups and that there was an increase in 6-*O* sulfation in the $Hs2st^{CKO}$ mutant.

Hs6st Genetically Interacts with Fgf10 in Lacrimal Gland Budding—Both human and mouse *Fgf10* mutations can cause lacrimal gland aplasia similar to that observed in $Hs6st^{CKO}$ newborn pups, suggesting that *Fgf10* may genetically interact with *Hs6st* in lacrimal gland development (41, 44). To test this idea, we crossed *Fgf10* with *Hs6st* mutant mice and collected embryos at E14.5. Although $Fgf10^{+/-}$ animals were previously reported to lack lacrimal gland at birth, we observed that these mutants retained either normal (3 of 12) or stunted (9 of 12) lacrimal gland buds at E14.5 (Fig. 3, *B* and *E*). The majority of the $Hs6st^{CKO}$ embryos (10 of 12) also exhibited some degree of lacrimal gland budding (Fig. 3, *C* and *E*; also Fig. 1*M*). In contrast, 10 of 12 $Fgf10^{+/-}$;$Hs6st^{CKO}$ embryos did not show any lacrimal gland buds (Fig. 3, *D* and *E*), strongly suggesting *Fgf10* and *Hs6st* operate in the same genetic pathway in lacrimal gland development.

Defective Fgf10 Signaling in the Hs2st and Hs6st Mutants—To investigate the mechanism of *Hs6st* function in Fgf10 signaling, we next carried out the LACE assay to examine the *in situ* binding of lacrimal gland heparan sulfate with Fgf10-Fgfr2b, the known FGF ligand/receptor pair in lacrimal gland development (23, 28). In the following experiments, we took care to select the *Hs2st*/*Hs6st* mutants that exhibited at least a small lacrimal gland bud, although similar results were also observed in the conjunctival epithelium from the more severe mutants that lacked any lacrimal gland budding (data not shown). As we have shown previously, soluble Fgf10 and Fgfr2b can bind the lacrimal gland sections through their interaction with endogenous heparan sulfate in wild type embryos (Fig. 4*A*). As a control, such binding was eliminated in sections pretreated with heparan sulfate-degrading enzyme heparitinase I (data not shown). Finally, Fgf10-Fgfr2b binding was weakened in the $Hs2st^{CKO}$ and the $Hs6st^{CKO}$ mutants and abolished in the $Hs2st^{CKO}$;$Hs6st^{CKO}$ mutants (Fig. 4, *B–D*, *arrow*), suggesting that heparan sulfate *O*-sulfation was essential for Fgf10-Fgfr2b interaction on lacrimal gland cell surface.

Fgf10 signaling is known to induce ERK phosphorylation and expression of *Erm* transcription factor in the lacrimal gland bud (28, 29). Although RNA *in situ* hybridization analysis showed that *Fgf10* and *Fgfr2b* expression were unchanged (data not shown), phospho-ERK and *Erm* levels were reduced in the $Hs2st^{CKO}$ and the $Hs6st^{CKO}$ mutants and completely lost in the remnants of the $Hs2st^{CKO}$;$Hs6st^{CKO}$ mutant buds (Fig. 4, *E–L*, *arrows*). Consistent with this finding, the $Hs2st^{CKO}$;$Hs6st^{CKO}$ mutants exhibited much reduced phosphohistone H3 (pHH3) labeling for cell proliferation and increasing TUNEL staining for apoptosis (Fig. 5, *A–J*). These results demonstrated that *Hs2st* and *Hs6st* mutations disrupted Fgf10-dependent downstream signaling and lacrimal gland outgrowth.

Combinatorial Contribution of Heparan Sulfate 2-O and 6-O Sulfation in Lacrimal Gland Fgf10 Signaling—Having established the importance of heparan sulfate 2-*O* and 6-*O* sulfation in lacrimal gland Fgf10 signaling, we next turned to the *Hs2st* and *Hs6st* MEF cells to extend our analysis to cellular level. MEF cells isolated from $Hs2st^{flox/flox}$ and $Hs6st1^{flox/flox}$;$Hs6st2^{-/-}$ embryos were first immortalized with a retrovirus expressing SV40 large T antigen followed by infection of a Cre-expressing adenovirus to convert the floxed alleles to null alleles. After clonal selection, the *Hs2st* and *Hs6st* null ($Hs2st^{-/-}$, $Hs6st^{-/-}$, and $Hs2st^{-/-}$;$Hs6st^{-/-}$) cells were propagated indefinitely in culture to ensure complete turnover of heparan sulfate that was present before adenoviral infection. As expected, disaccharide analysis of heparan sulfate from $Hs2st^{-/-}$ cells showed a complete loss of disaccharides containing 2-*O*-sulfate groups (D2H6, D2A0, D2S0, and D2S6) but an increased amount of the 6-*O* sulfated unit, D0S6, resulting in a slight overall increase in the amount of 6-O-sulfate groups (Fig. 6, *A* and *B*). Heparan sulfate in $Hs6st^{-/-}$ cells showed complete elimination of 6-*O*-sulfation (D0A6, D0S6, and D2S6). There was a corresponding increase in D2A0 and D2S0, resulting in a moderate increase in overall 2-*O* sulfation (Fig. 6, *A* and *B*). In the $Hs2st^{-/-}$;$Hs6st^{-/-}$ cells, complete loss of *O*-sulfated disaccharides was accompanied by a striking increase in *N*-sulfation (D0S0). Less dramatic increases in *N*-sulfation were noted in each of the single

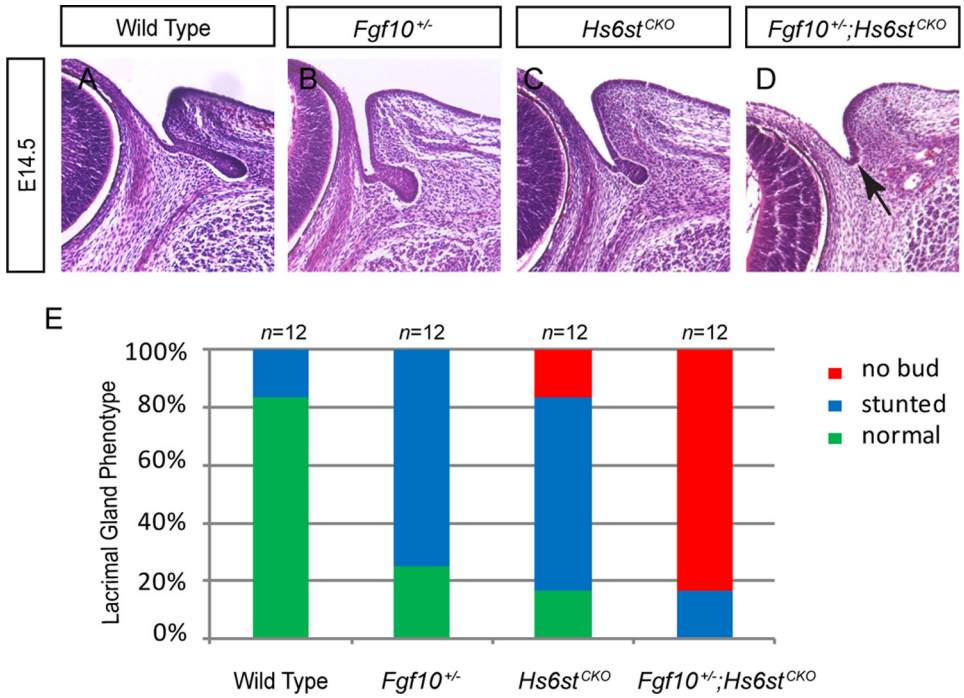

FIGURE 3. **Genetic interaction between *Hs6st* and *Fgf10*.** *A–D*, lacrimal gland bud was present in both $Fgf10^{+/-}$ and $Hs6st^{CKO}$ mutants at E14.5 but lost in the $Fgf10^{+/-};Hs6st^{CKO}$ compound mutants (*arrow*). *E*, quantification of the lacrimal gland phenotype is shown.

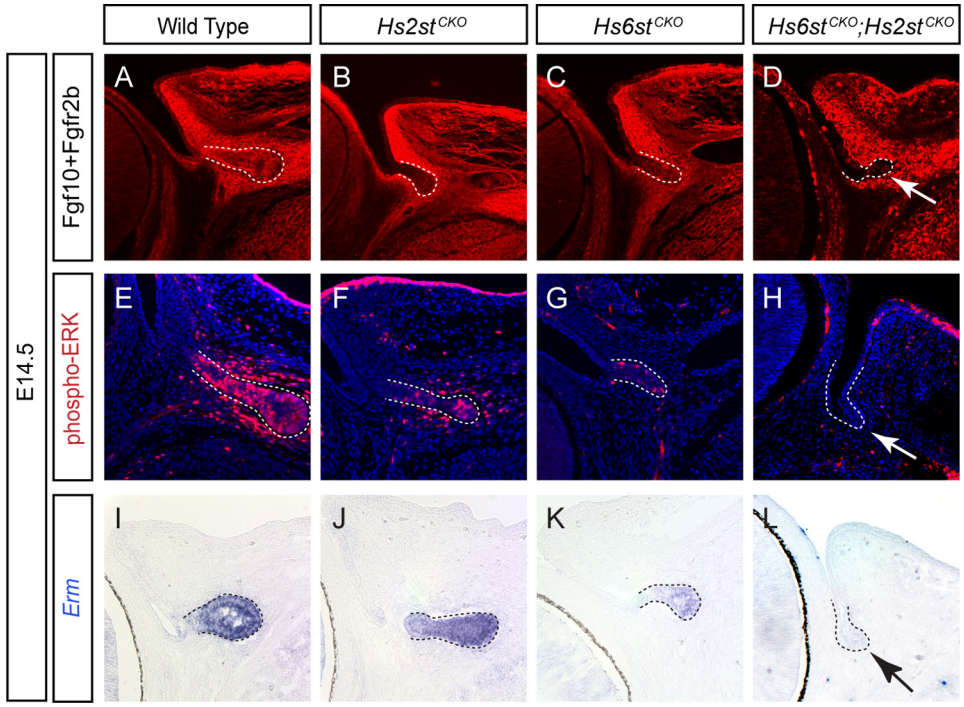

FIGURE 4. **Hs2st/*Hs6st* mutants disrupted Fgf10/Fgfr2b signaling in lacrimal gland development.** *A–D*, *in situ* binding (LACE assay) of Fgf10/Fgfr2b on lacrimal gland sections were reduced in the $Hs2st^{CKO}$ and $Hs6st^{CKO}$ single mutants and abolished in the $Hs2st^{CKO};Hs6st^{CKO}$ double mutants (*arrow*). *E–L*, downstream of FGF signaling, phospho-ERK and *Erm* expression was also reduced in the $Hs2st^{CKO}$ and $Hs6st^{CKO}$ single mutants and lost in the $Hs2st^{CKO};Hs6st^{CKO}$ double mutants (*arrow*).

mutants as well (Fig. 6*B*). When total sulfation of heparan sulfate was determined by summation of *N*- and *O*-sulfates, the overall level of sulfation did not differ significantly in the single and double mutants compared with wild type (Fig. 6*B*). In general, the alterations in heparan sulfate composition in the fibroblasts resembled the changes inferred by *in situ* assay of tissue sections from the lacrimal gland with single chain antibodies (Fig. 2). We next examined Fgf10 signaling in the $Hs2st^{-/-}$ and $Hs6st^{-/-}$ cells by measuring its downstream ERK phosphorylation. As shown by quantitative Western blot, wild type MEF cells responded to Fgf10 stimulation with a rapid increase in ERK phosphorylation, whereas the peak level of such response was only slightly reduced in the $Hs2st^{-/-}$ and $Hs6st^{-/-}$ cells (Fig. 6, *C* and *D*). Importantly, the $Hs2st^{-/-};Hs6st^{-/-}$ cells

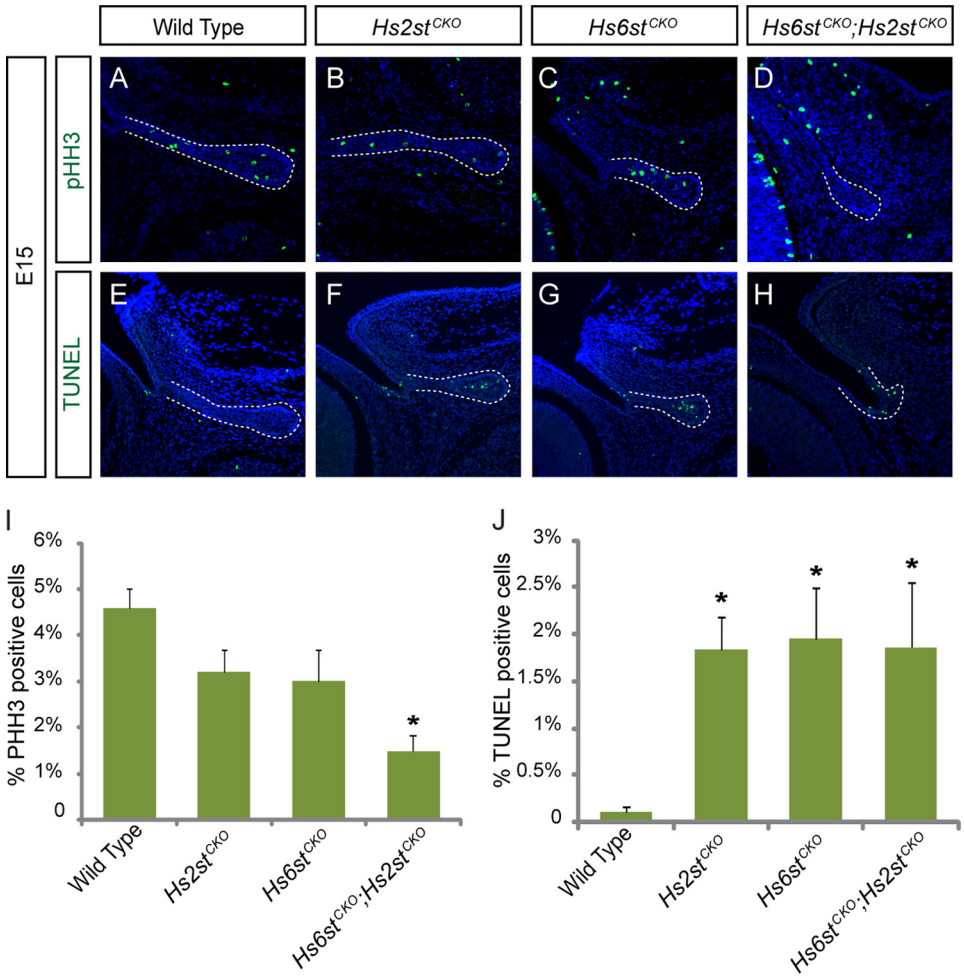

FIGURE 5. **Cell proliferation and apoptosis defects in the *Hs2st*/*Hs6st* mutants.** *A–D*, the *Hs2st*^{CKO};*Hs6st*^{CKO} mutants exhibited reduced expression of cell proliferation marker phosphohistone H3 (pHH3). *E–H*, although the wild type control lacrimal gland showed no TUNEL staining, all *Hs2st*^{CKO} and *Hs6st*^{CKO} mutant lacrimal gland primordia contained TUNEL-positive cells. *I* and *J*, quantification of phosphohistone H3 and TUNEL staining (*, $p < 0.01$).

exhibited dramatic reduction in Fgf10 response, consistent with the critical role of heparan sulfate 2-*O* and 6-*O* sulfations in Fgf10 signaling.

Finally, we performed explant culture experiments to assay Fgf10 signaling response directly in the *Hs2st* and *Hs6st* lacrimal glands. After culturing for 2 days, wild type eye rudiments readily grew endogenous lacrimal glands, which were unperturbed by BSA-soaked beads (Fig. 7*A*, *arrow*). Ectopic lacrimal gland budding, however, was only observed in response to Fgf10-soaked beads implanted around the eye (Fig. 7*B*, *arrowhead*). Interestingly, Fgf10 beads also induced ectopic lacrimal glands in the *Hs2st*^{CKO} and the *Hs6st*^{CKO} explants, suggesting that these mutants could still respond to high levels of exogenous Fgf10. In contrast, both endogenous and ectopic lacrimal gland budding were lost in the *Hs2st*^{CKO};*Hs6st*^{CKO} mutant cultures ($p = 0.0005$, Fisher's test). Therefore, ablations of both Hs2st and Hs6st activities were necessary to completely abolish Fgf10 signaling in lacrimal gland budding.

DISCUSSION

All cells synthesize heparan sulfate and, therefore, must express at least a core set of biosynthetic enzymes required for chain polymerization (Ext1, Ext2, and Extl3), and processing (one or more Ndsts, Hsepi, and Hs2st and one or more Hs6sts and Hs3sts). However, it has long been recognized that the levels of the various enzymes are expressed in a dynamic pattern in different tissues. For example, *Hs6st1* is strongly expressed in epithelial cells, whereas *Hs2st* and *Hs6st2* are found expressed more strongly in mesenchymal compartments (18, 34). It is, therefore, surprising that the *Hs6st1* systemic knockouts lack major organogenesis defects, *Hs6st2* and *Ndst2* mice are viable and fertile (19–21), and mutants altered in *Ndst1* or *Hs2st* exhibit specific organ and tissue abnormalities. These observations suggest that heparan sulfate, although essential for organismal growth and development, plays different roles in different tissues.

It has been known since 1991 that members of the FGF family of growth factors and their receptors interact with heparan sulfate, which serves as a coreceptor by facilitating the formation and stability of FGF-FGFR complexes. Despite extensive biochemical studies in support of a role for heparan sulfate in FGF signaling, none of the murine *Hs2st* and *Hs6st* knock-out phenotypes has been conclusively attributed to FGF signaling defects. We previously showed that lacrimal gland development requires specific modification of heparan sulfates by *Ndst* genes in the epithelial cells at the tip of the lacrimal gland bud.

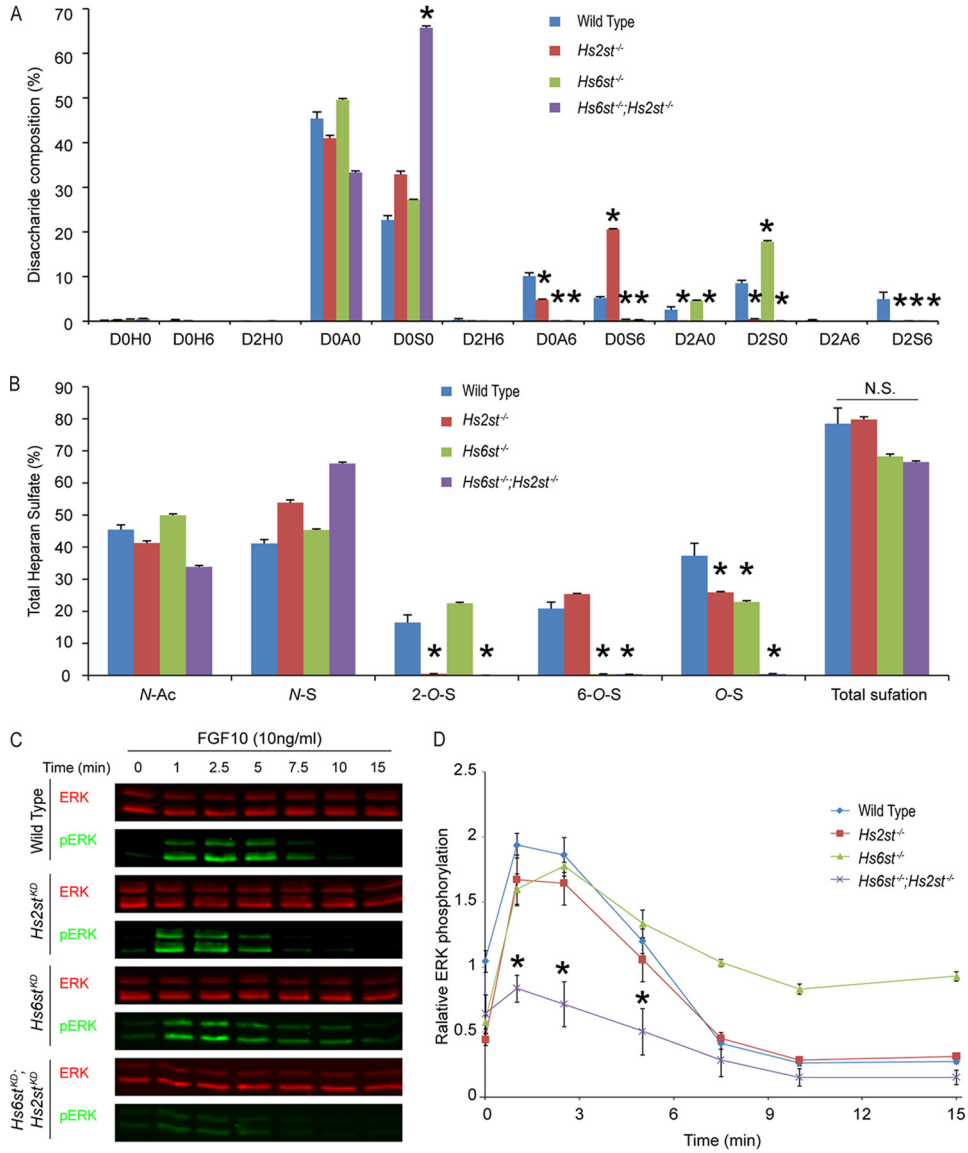

FIGURE 6. **Disruption of Fgf10 signaling in the *Hs6st/Hs2st* knock-out MEF cells.** *A*, immortalized MEF cells were clonally selected to generate the *Hs2st* and *Hs6st* null (*Hs2st*$^{-/-}$, *Hs6st*$^{-/-}$, and *Hs2st*$^{-/-}$;*Hs6st*$^{-/-}$) cells. The disaccharide composition of heparan sulfate derived from the cells was determined by enzymatic depolymerization and liquid chromatography/mass spectrometry. Each disaccharide is defined by a structure code: *D0H0*, ΔUA-GlcNH$_2$; *D0H6*, ΔUA-GlcNH$_2$-6S; *D2H0*, ΔUA2S-GlcNH$_2$; *D0A0*, ΔUA-GlcNAc; *D0S0*, ΔUA-GlcNS; *D2H6*, ΔUA2S-GlcNH$_2$6S; *D0A6*, ΔUA-GlcNAc6S; *D0S6*, ΔUA-GlcNS6S; *D2A0*, ΔUA2S-GlcNAc; *D2S0*, ΔUA2S-GlcNS; *D2A6*, ΔUA2S-GlcNAc6S; *D2S6*, ΔUA2S-GlcNS6S, where ΔUA = 4,5-unsaturated uronic acid generated during the heparin lyase reaction (47). *, one-way analysis of variance: $p < 0.05$ for the comparison with the wild type. The data reflected three independent experiments for each cell line and were confirmed in two independently cloned cells for each genotype. *B*, the amount of *N*-acetyl groups and sulfate groups at various positions was calculated from the data in *panel A*. *, one-way analysis of variance: $p < 0.05$ for the comparison with the wild type; *N.S.*, not significant. *C*, the *Hs2st* and *Hs6st* knock-out MEF cells were stimulated with 10 ng/ml Fgf10, and the time course of ERK phosphorylation was determined by fluorescent Western blot. *D*, the relative level of phospho-ERK was significantly reduced in the *Hs2s*$^{-/-}$;*Hs6st*$^{-/-}$ cells. Three independent experiments were performed for each cell line, and the results were confirmed in two independently cloned cells for each genotype. *, $p < 0.01$ for the comparison with the wild type.

In this system, Ndst1-modified heparan sulfate serves as a coreceptor enabling the formation of Fgf10-Fgfr2b complexes and downstream signaling via phosphorylation of Shp2 and Erk. Reduction of Ndst1 causes reduced *N*-sulfation, which is prerequisite for all downstream reactions, including 2-*O*-sulfation and 6-*O*-sulfation. Thus, the role of *O*-sulfation in Fgf10-Fgfr2b signaling and lacrimal gland development remained an open question.

In this study we have generated combinatorial ablations of *Hs2st*, *Hs6st1*, and *Hs6st2* in the lacrimal gland, which led to specific loss of heparan sulfate 2-*O* or 6-*O* sulfation and distinct developmental defects. In support of heparan sulfate *O*-sulfation in promoting FGF signaling, we showed that loss of Hs6st decreased lacrimal gland development and that *Hs6st1* genetically interacted with *Fgf10* in lacrimal gland budding. Because 2-*O*-sulfation increases somewhat in the absence of Hs6st, the contribution of 6-*O*-sulfation may be somewhat underestimated. Compounding the mutants resulted in complete loss of signaling and potentiated the loss of lacrimal gland development. Furthermore, *Hs2st*/*Hs6st* mutations disrupted cell surface Fgf10-Fgf2b assembly and downstream ERK signaling. The profound effect of compounding these mutations suggests that both 2-*O*-sulfation and 6-*O*-sulfation of heparan sulfate contribute to Fgf10-Fgfr2b signaling. To our knowledge, this is the

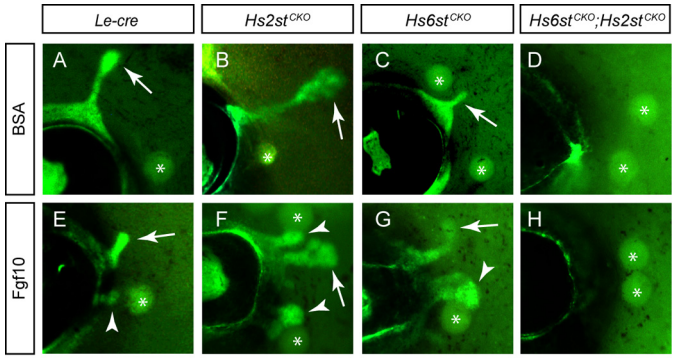

I

		Lacrimal gland budding rate (%)		
		Endogenous	Ectopic	(# of explants)
Le-cre	BSA	60%	0%	(10)
	Fgf10	46%	31%	(29)
Hs2st^{CKO}	Fgf10	50%	28%	(18)
Hs6st^{CKO}	Fgf10	31%	21%	(62)
Hs6st^{CKO};Hs2st^{CKO}	Fgf10	0%	0%	(33)

FIGURE 7. **Fgf10 requires *Hs6st/Hs2st* to induce lacrimal gland budding *ex vivo*.** *A–H*, although implantation of BSA beads did not affect endogenous lacrimal gland budding (*arrows*), Fgf10-soaked beads induced ectopic lacrimal gland buds in wild type control, *Hs2st^{CKO}*, and *Hs6st^{CKO}* explants (*arrowheads*). However, no lacrimal gland buds were observed in the *Hs2st^{CKO};Hs6st^{CKO}* mutant explants. * denotes implanted beads. *I*, the lacrimal gland budding rate for each *Hs6st/Hs2st* mutant is shown.

first study to show that simultaneous deletion of *Hs2st* and *Hs6st* exhibits profound FGF signaling defects in mammalian development.

In *Drosophila* trachea branching morphogenesis, Kamimura *et al.* (17) have previously shown that *Hs2st* and *Hs6st* single mutants abolished the corresponding sulfation reactions, but the charge density of *Drosophila* heparan sulfate remained constant due to increases in sulfation at other positions. Because FGF signaling was unaffected in *Hs2st* and *Hs6st* single mutants but abolished in *Hs2st*/*Hs6st* double mutants, these authors concluded that the function of heparan sulfate depends on the absolute amount but not the specific pattern of sulfation. According to this model, mutant heparan sulfate chains should support FGF signaling as long as they maintain normal levels of overall sulfation (17). Mechanistically, any model must take into account the fact that the binding of ligands to heparan sulfate usually occurs via a short oligosaccharide of ~5–12 residues (12, 45). Thus, compensation can take place only if the binding sites for heparan sulfate in the ligand and/or the receptor can accommodate sulfate groups located at different positions and the heparan sulfate chain can reorient to position the sulfate groups appropriately. Structural studies of Fgf10-Fgfr2b complexes with defined heparan sulfate oligosaccharides are needed to critically evaluate this issue.

As in other systems, deletion of *O*-sulfotransferases involved in heparan sulfate processing results in enhanced sulfation at other positions. Thus, deletion of *Hs2st* in CHO cells, *Drosophila*, and mice results in enhanced *N*-sulfation and 6-*O*-sulfation, whereas deletion of *Hs6st* results in increased *N*-sulfation and 2-*O*-sulfation. The mechanism that underlies these changes is unknown and might reflect intrinsic properties of the enzymes with respect to substrate preference. Alternatively, changes in the level of expression or organization of the biosynthetic enzymes might occur. In either case, the assembly process appears to be coordinated to buffer changes in composition, which in turn prevents deleterious effects on receptor signaling, at least in the context of FGF reception. Whether these changes in heparan sulfate structure also result in activation or repression of other signaling systems is an interesting possibility that should be considered.

Given the large number of FGF and FGFR family members (46) and variation in the amount and composition of heparan sulfate expressed in different cells and tissues, it is not surprising that the requirement for heparan sulfate might vary considerably for different FGFs and FGF receptors. Here, we show a preference for 6-*O*-sulfate groups with contribution of 2-*O*-sulfate groups for FGF10-FGFR2b signaling that enables lacrimal gland development. Our findings are consistent with prior binding studies showing a requirement for 6-*O*-sulfation for oligosaccharide binding to Fgf10 but differ in that 2-*O*-sulfate groups were dispensable for binding (22). Presumably, the different results reflect the experimental systems under study and emphasize the importance of evaluating these interactions *in vivo* to determine the biological relevance of biochemical measurements.

Acknowledgments—We thank Drs. Ruth Ashley-Padan, Bridget Hogan, Richard Lang, Lawrence Quilliam, and Hisashi Umemori for mice and reagents and members of the Zhang laboratory for discussions.

REFERENCES

1. Häcker, U., Nybakken, K., and Perrimon, N. (2005) *Nat. Rev. Mol. Cell Biol.* **6,** 530–541
2. Lin, X. (2004) *Development* **131,** 6009–6021
3. Ori, A., Wilkinson, M. C., and Fernig, D. G. (2008) *Front. Biosci.* **13,** 4309–4338
4. Esko, J. D., and Selleck, S. B. (2002) *Annu. Rev. Biochem.* **71,** 435–471
5. Guimond, S. E., and Turnbull, J. E. (1999) *Curr. Biol.* **9,** 1343–1346
6. Li, J. P., Gong, F., Hagner-McWhirter, A., Forsberg, E., Abrink, M., Kisilevsky, R., Zhang, X., and Lindahl, U. (2003) *J. Biol. Chem.* **278,** 28363–28366
7. Merry, C. L., Bullock, S. L., Swan, D. C., Backen, A. C., Lyon, M., Beddington, R. S., Wilson, V. A., and Gallagher, J. T. (2001) *J. Biol. Chem.* **276,** 35429–35434
8. Ostrovsky, O., Berman, B., Gallagher, J., Mulloy, B., Fernig, D. G., Delehedde, M., and Ron, D. (2002) *J. Biol. Chem.* **277,** 2444–2453
9. Pye, D. A., Vives, R. R., Turnbull, J. E., Hyde, P., and Gallagher, J. T. (1998) *J. Biol. Chem.* **273,** 22936–22942
10. Wu, Z. L., Zhang, L., Yabe, T., Kuberan, B., Beeler, D. L., Love, A., and Rosenberg, R. D. (2003) *J. Biol. Chem.* **278,** 17121–17129
11. Jastrebova, N., Vanwildemeersch, M., Lindahl, U., and Spillmann, D. (2010) *J. Biol. Chem.* **285,** 26842–26851
12. Kreuger, J., Spillmann, D., Li, J. P., and Lindahl, U. (2006) *J. Cell Biol.* **174,** 323–327
13. Bülow, H. E., and Hobert, O. (2006) *Annu. Rev. Cell Dev. Biol.* **22,** 375–407
14. Lindahl, U., and Li, J. P. (2009) *Int. Rev. Cell Mol. Biol.* **276,** 105–159
15. Jastrebova, N., Vanwildemeersch, M., Rapraeger, A. C., Giménez-Gallego, G., Lindahl, U., and Spillmann, D. (2006) *J. Biol. Chem.* **281,** 26884–26892
16. Kreuger, J., Jemth, P., Sanders-Lindberg, E., Eliahu, L., Ron, D., Basilico, C., Salmivirta, M., and Lindahl, U. (2005) *Biochem. J.* **389,** 145–150
17. Kamimura, K., Koyama, T., Habuchi, H., Ueda, R., Masu, M., Kimata, K.,

and Nakato, H. (2006) *J. Cell Biol.* **174,** 773–778
18. Bullock, S. L., Fletcher, J. M., Beddington, R. S., and Wilson, V. A. (1998) *Genes Dev.* **12,** 1894–1906
19. Habuchi, H., Nagai, N., Sugaya, N., Atsumi, F., Stevens, R. L., and Kimata, K. (2007) *J. Biol. Chem.* **282,** 15578–15588
20. Izvolsky, K. I., Lu, J., Martin, G., Albrecht, K. H., and Cardoso, W. V. (2008) *Genesis* **46,** 8–18
21. Sugaya, N., Habuchi, H., Nagai, N., Ashikari-Hada, S., and Kimata, K. (2008) *J. Biol. Chem.* **283,** 10366–10376
22. Ashikari-Hada, S., Habuchi, H., Kariya, Y., Itoh, N., Reddi, A. H., and Kimata, K. (2004) *J. Biol. Chem.* **279,** 12346–12354
23. Allen, B. L., and Rapraeger, A. C. (2003) *J. Cell Biol.* **163,** 637–648
24. Nagai, N., Habuchi, H., Kitazume, S., Toyoda, H., Hashimoto, Y., and Kimata, K. (2007) *J. Biol. Chem.* **282,** 14942–14951
25. Pratt, T., Conway, C. D., Tian, N. M., Price, D. J., and Mason, J. O. (2006) *J. Neurosci.* **26,** 6911–6923
26. Patel, V. N., Likar, K. M., Zisman-Rozen, S., Cowherd, S. N., Lassiter, K. S., Sher, I., Yates, E. A., Turnbull, J. E., Ron, D., and Hoffman, M. P. (2008) *J. Biol. Chem.* **283,** 9308–9317
27. Stanford, K. I., Wang, L., Castagnola, J., Song, D., Bishop, J. R., Brown, J. R., Lawrence, R., Bai, X., Habuchi, H., Tanaka, M., Cardoso, W. V., Kimata, K., and Esko, J. D. (2010) *J. Biol. Chem.* **285,** 286–294
28. Pan, Y., Woodbury, A., Esko, J. D., Grobe, K., and Zhang, X. (2006) *Development* **133,** 4933–4944
29. Pan, Y., Carbe, C., Powers, A., Zhang, E. E., Esko, J. D., Grobe, K., Feng, G. S., and Zhang, X. (2008) *Development* **135,** 301–310
30. Min, H., Danilenko, D. M., Scully, S. A., Bolon, B., Ring, B. D., Tarpley, J. E., DeRose, M., and Simonet, W. S. (1998) *Genes Dev.* **12,** 3156–3161
31. Ashery-Padan, R., Marquardt, T., Zhou, X., and Gruss, P. (2000) *Genes Dev.* **14,** 2701–2711
32. Cai, Z., Feng, G. S., and Zhang, X. (2010) *J. Neurosci.* **30,** 4110–4119
33. van Kuppevelt, T. H., Dennissen, M. A., van Venrooij, W. J., Hoet, R. M., and Veerkamp, J. H. (1998) *J. Biol. Chem.* **273,** 12960–12966
34. Sedita, J., Izvolsky, K., and Cardoso, W. V. (2004) *Dev. Dyn.* **231,** 782–794
35. Jat, P. S., Cepko, C. L., Mulligan, R. C., and Sharp, P. A. (1986) *Mol. Cell. Biol.* **6,** 1204–1217
36. Li, Y., Yan, J., De, P., Chang, H. C., Yamauchi, A., Christopherson, K. W., 2nd, Paranavitana, N. C., Peng, X., Kim, C., Munugalavadla, V., Munugulavadla, V., Kapur, R., Chen, H., Shou, W., Stone, J. C., Kaplan, M. H., Dinauer, M. C., Durden, D. L., and Quilliam, L. A. (2007) *J. Immunol.* **179,** 8322–8331
37. Lawrence, R., Olson, S. K., Steele, R. E., Wang, L., Warrior, R., Cummings, R. D., and Esko, J. D. (2008) *J. Biol. Chem.* **283,** 33674–33684
38. Makarenkova, H. P., Hoffman, M. P., Beenken, A., Eliseenkova, A. V., Meech, R., Tsau, C., Patel, V. N., Lang, R. A., and Mohammadi, M. (2009) *Sci. Signal.* **2,** ra55
39. Pan, Y., Carbe, C., Powers, A., Feng, G. S., and Zhang, X. (2010) *Development* **137,** 1085–1093
40. Govindarajan, V., Ito, M., Makarenkova, H. P., Lang, R. A., and Overbeek, P. A. (2000) *Dev. Biol.* **225,** 188–200
41. Makarenkova, H. P., Ito, M., Govindarajan, V., Faber, S. C., Sun, L., McMahon, G., Overbeek, P. A., and Lang, R. A. (2000) *Development* **127,** 2563–2572
42. Jenniskens, G. J., Oosterhof, A., Brandwijk, R., Veerkamp, J. H., and van Kuppevelt, T. H. (2000) *J. Neurosci.* **20,** 4099–4111
43. Dennissen, M. A., Jenniskens, G. J., Pieffers, M., Versteeg, E. M., Petitou, M., Veerkamp, J. H., and van Kuppevelt, T. H. (2002) *J. Biol. Chem.* **277,** 10982–10986
44. Entesarian, M., Matsson, H., Klar, J., Bergendal, B., Olson, L., Arakaki, R., Hayashi, Y., Ohuchi, H., Falahat, B., Bolstad, A. I., Jonsson, R., Wahren-Herlenius, M., and Dahl, N. (2005) *Nat. Genet.* **37,** 125–127
45. Selleck, S. B. (2000) *Trends Genet.* **16,** 206–212
46. Ornitz, D. M. (2000) *Bioessays* **22,** 108–112
47. Lawrence, R., Lu, H., Rosenberg, R. D., Esko, J. D., and Zhang, L. (2008) *Nat. Methods* **5,** 291–292